Max-Planck-Institut für Mathematik
Bonn

A novel discontinuous Galerkin method using the principle of discrete least squares

by

Jan Glaubitz
Philipp Öffner

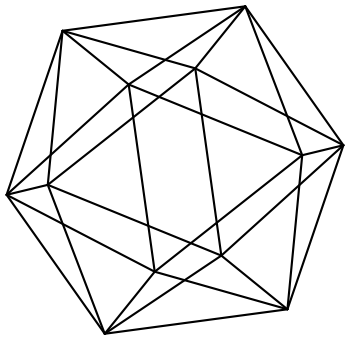

Max-Planck-Institut für Mathematik
Preprint Series 2017 (63)

A novel discontinuous Galerkin method using the principle of discrete least squares

Jan Glaubitz
Philipp Öffner

Max-Planck-Institut für Mathematik
Vivatsgasse 7
53111 Bonn
Germany

Institut Computational Mathematics
TU Braunschweig
Universitätsplatz 2
38106 Braunschweig
Germany

MPIM 17-63

A novel discontinuous Galerkin method using the principle of discrete least squares

Jan Glaubitz*and Philipp Öffner†

October 16, 2017

In this work, a novel discontinuous Galerkin (DG) method is introduced by utilising the principle of discrete least squares. The key idea is to build polynomial approximations by the method of (weighted) discrete least squares instead of usual interpolation or (discrete) L^2 projections. The resulting method hence uses more information of the underlying function and provides a more robust alternative to common DG methods. As a result, we are able to construct high-order schemes which are conservative as well as linear stable on *any* set of collocation points. Several numerical tests highlight the new *discontinuous Galerkin discrete least squares (DG-DLS)* method to significantly outperform present-day DG methods.

MSC2010: 35L65, 65M60, 93E24, 33C47
Keywords: Hyperbolic conservation laws, high order methods, discontinuous Galerkin methods, least squares, discrete orthogonal polynomials

1. Introduction

In the last decades, great efforts have been made to develop accurate and stable numerical methods for time dependent partial differential equations (PDEs), especially for hyperbolic conservation laws $\partial_t u + \partial_x f(u) = 0$. Traditionally, low order numerical schemes, for instance finite volume (FV), have been used to solve hyperbolic conservation laws, particularly in industrial applications. Since they become quite costly for high accuracy or long time simulations, however, there is a rising demand of high order (third and above) methods. These have the potential of providing accurate solutions at reasonable costs. Yet, high order methods most often are less robust and specific distributions of points for the numerical integration and polynomial interpolation of the solution have to be used. This entails, for instance, that present-day high order methods, such as the discontinuous Galerkin collocation spectral element method (DGSEM) of Gassner and Kopriva [3, 4, 16] and flux reconstruction (FR) [14, 22] method, heavily rely on Gauss-Legendre (GLe) or Gauss-Lobatto (GLo) points. The need to improve existing high-order methods as well as to develop new ones with more favourable properties is therefore a crucial task and has attracted interest of many researchers.

The current work is a step in this direction. A novel high order discontinuous Galerkin (DG) method for hyperbolic conservation laws is introduced by using the principle of discrete least squares, i.e. discrete orthogonal polynomial least squares (DOP-LS) approximations.

*Max-Planck-Institut für Mathematik, Vivatsgasse 7, 53111 Bonn, Germany.
Institut Computational Mathematics, TU Braunschweig, Universitätsplatz 2, 38106 Braunschweig, Germany.
(j.glaubitz@tu-bs, https://www.tu-braunschweig.de/icm/pde/personal/jglaubitz)
†Institut Computational Mathematics, TU Braunschweig, Universitätsplatz 2, 38106 Braunschweig, Germany.
(p.oeffner@tu-bs, https://www.tu-braunschweig.de/icm/pde/personal/poeffner)

For one spatial dimension, in a high order semidiscretisation of conservation laws, the solution is approximated in each element by an (interpolation) polynomial of degree K. This polynomial, usually referred to as the *solution polynomial*, is constructed by using the data at $K+1$ (interpolation) points. In order to achieve high orders of accuracy - and not to run into the Runge phenomenon - one has to restrict to very specific point distributions, most commonly Gauss-Legendre and Gauss-Lobatto points. Equidistant points are the worst case scenario from this point of view.

Our new method tackles this problem by making a somewhat maverick generalisation. Instead of the usual polynomial approximation by interpolation on $K+1$ points, we build them by the method of discrete least squares (DLS), where now the data at $N > K+1$ points is used. The method thus utilises more information from the underlying function. By going over to a higher number of nodal values than technically needed, polynomial DLS approximations are known to provide high accuracy while also successfully suppressing Runge oscillations, even on equidistant points.

This generalisation does not only allow us to utilise completely new tools, but also to formulate the new method on any geometry and set of collocation points. We demonstrate this, by especially focusing on equidistant points. Since the DOP-LS approximation extends the common polynomial interpolation, the method provides a generalisation of brought classes of existing DG methods, particularly of the recent discontinuous Galerkin collocation spectral element method (DGSEM) of Gassner and Kopriva [3, 4, 16].

To the best of our knowledge, this is the first time, DOP-LS approximations are incorporate into a DG method, or any other (spectral element) hp-method for hyperbolic conservation laws. In [8], the authors applied the DOP-LS approximation based on the super Gaussian weight function as a hybrid spectral method on the whole computational domain. It should be stressed, however, that this approach fails formidably when transferred to the problems and numerical method addressed in this work. As we shall see later, when incorporated into a DG method, the DOP-LS approximation needs to be based on very specific weights. Utilising these, we are then able to proof conservation as well as linear stability of our novel DG method on any point distribution.

Our discussion begins by briefly revisiting the idea of DG methods in section 2. This revision, in particular, is based on the recent DGSEM. Utilising the idea of collocation, we will explain the incorporation of DOP-LS approximations based on the DGSEM. Before doing so, however, discrete orthogonal polynomials and the principle of discrete least squares are introduced in section 3. By the Stieltjes recurrence relation, we are able to construct a basis of orthogonal polynomials to every (discrete) weight function. Orthogonal basis functions for instance yield a diagonal mass matrix and therefore a significantly more efficient DG method. Similar to the (Legendre-)Fourier-projection, the coefficients of the DOP-LS approximation can furthermore be computed highly efficient by evaluating an inner product, where the integral is now replaced by a simple finite sum. In section 4, the DOP-LS approximation is then introduced in a DG method, replacing the common polynomial interpolation by a discrete least squares approximation. The resulting novel DG method is referred to as the *discontinuous Galerkin discrete least squares (DG-DLS)* method and generalises brought classes of existing DG methods. Conservation as well as linear stability of the new DG-DLS method are proven in section 5. While this work mainly focuses on equally distributed points in the numerical tests, both properties are shown to hold on any set of collocation points. The key point is solely the 'right' choice of discrete weights, in order to provide quadrature rules of sufficiently high order. Numerical tests and an error as well as convergence analysis are provided in section 6. Section 7 summarises the distinctive features of the new DG-DLS method and further discusses future research and applications.

2. A Discontinuous Galerkin method

Discontinuous Galerkin (DG) methods for hyperbolic conservation laws, $\partial_t u + \partial_x f(u) = 0$, are constructed by the idea to approximate the conservation variable(s) u as well as the flux f by certain polynomials u_K, f_K of degree K or less. Subsequently, the corresponding residual

$$\mathcal{R}_K = \partial_t u_K + \partial_x f_K \tag{1}$$

is demanded to vanish in the sense that it should be orthogonal to the approximation space $\mathbb{P}_K$, i.e.

$$\langle \mathcal{R}_K, \psi \rangle_{L^2_\omega} = \int_{-1}^{1} (\partial_t u_K + \partial_x f_K)\, \psi \omega = 0 \quad \forall \psi \in \mathbb{P}_K \tag{2}$$

on a reference element $\Omega_{ref} = [-1, 1]$ and with weight function $\omega : [-1, 1] \to \mathbb{R}_0^+$.

Typically, u_K and f_K are interpolation polynomials associated to a given set of interpolation points. Orthogonality is further meant with respect to a common L^2 norm ($\omega = 1$), which often is approximated by a quadrature rule using the same points as for the interpolation then. This idea to match the interpolation points for the approximations u_K, f_K also with the quadrature rule is commonly known as the *collocation approach*.

For highest accuracy in both, polynomial interpolation as well as numerical integration, typically Gauss or Gauss-Lobatto points are used. These are more dense at the boundaries and thus prevent spurious oscillations due to the Runge phenomenon. In [8,18], notably harsh time step restrictions have been pointed out to arise from collocation points which are more dense at certain areas. In our opinion, there are farther drawbacks of present-day DG schemes, which will therefore be addressed in subsection 2.2. Before doing so, we want to give a specific example for a DG method using a collocation approach, namely the *discontinuous Galerkin collocation spectral element method* (DGSEM). This is done in the prior subsection 2.1 in a less abstract and thus more detailed way then the above description. It will further be the DGSEM we will explain our novel DOP-LS approach for in section 3.

2.1. The Discontinuous Galerkin collocation spectral element method

Decoupling space and time by the method of lines [19], DG methods are designed as semidiscretisations of hyperbolic conservation laws,

$$\partial_t U + \nabla \cdot F(U) = 0, \tag{3}$$

on a computational domain Ω. Thereby, the vector $U = \left[u^1(t,x), \ldots, u^d(t,x)\right]^T$ is referred to as the *vector of conservation variables* and $F(U) = \left[f^1(U), \ldots, f^s(U)\right]^T$ is referred to as the *flux*. Combining ideas from finite volume (FV) as well as spectral methods, first of all, the computational domain Ω is subdivided into nonoverlapping elements $\Omega_i, i \in I$.

In one space dimension, each element is mapped to a reference element $\Omega_{ref} = [-1, 1]$ by

$$x(\xi) = \overline{x} + \frac{\Delta x}{2}\xi, \tag{4}$$

where $\overline{x}$ is the centre of the element and Δx its length. In the same way, equation (3) is transformed into the reference space,

$$\frac{\Delta x}{2}\partial_t U + \partial_\xi F(U) = 0, \tag{5}$$

where all computations are performed then. The extension to multiple dimensions can for instance be achieved by tensor products.

In the following, a DG discretisation using a collocation spectral element method (DGSEM) is reviewed for a scalar conservation law $\partial_t u + \partial_x f(u) = 0$. For systems, the procedure is simply applied to every conservation variable separately.

The DG method now uses a polynomial approximation of the conservation variable u of degree K or less in the reference element $\Omega_{ref} = [-1, 1]$. Typically, the interpolation polynomial with respect to $K + 1$ interpolation points $\{\xi_j\}_{j=0}^K$ is utilised, i.e.

$$u(t,x)\big|_{\Omega_i} \approx u_K(t,\xi) = \sum_{k=0}^{K} u_k(t) l_k(\xi), \tag{6}$$

where $u_k(t) = u(t, \xi_k)$ are the time depended nodal values at the interpolation points and l_k are the corresponding Lagrange basis functions defined by

$$l_k(\xi) = \prod_{j=0, j\neq k}^{K} \frac{\xi - \xi_j}{\xi_k - \xi_j}, \tag{7}$$

and satisfying the cardinal property $l_k(\xi_j) = \delta_{kj}$. The same polynomial approximation is also used for the flux, which is thus replaced by

$$f(u)\big|_{\Omega_i} \approx f_K(t, \xi) = \sum_{k=0}^{K} f_k(t) l_k(\xi). \tag{8}$$

Here, the idea of collocation is used to determine the nodal values of the flux, i.e.

$$f_k(t) = f(u_k(t)), \quad k = 0, \dots, K, \tag{9}$$

which means that the flux is approximated by an interpolation polynomial as well, further using the same interpolation points $\{\xi_k\}_{k=0}^K$. Finally, both polynomial approximations can be inserted into the transformed equation (5), yielding

$$\frac{\Delta x}{2} \partial_t u_K(t, \xi) + \partial_x f_K(t, \xi) = 0 \tag{10}$$

on the reference element Ω_{ref}. Multiplying by a test function l_i, $i = 0, \dots, K$, and integrating over the reference element element, $K + 1$ equations

$$\int_{-1}^{1} \left(\frac{\Delta x}{2} \partial_t u_K + \partial_\xi f_K \right) l_i \, \mathrm{d}\, \xi = 0, \quad i = 0, \dots, K \tag{11}$$

arise. Applying integration by parts once, the locally defined weak form

$$\int_{-1}^{1} \frac{\Delta x}{2} \left(\partial_t u_K \right) l_i \, \mathrm{d}\, \xi - \int_{-1}^{1} f_K \left(\partial_\xi l_i \right) \mathrm{d}\, \xi = - \left(f_R^{\mathrm{num}} l_i(1) - f_L^{\mathrm{num}} l_i(-1) \right), \quad i = 0, \dots, K, \tag{12}$$

is recovered, and by applying integration by parts a second time, the locally defined strong form

$$\int_{-1}^{1} \left(\frac{\Delta x}{2} \partial_t u_K + \partial_\xi f_K \right) l_i \, \mathrm{d}\, \xi = \left(f_K(1) - f_R^{\mathrm{num}} \right) l_i(1) - \left(f_K(-1) - f_L^{\mathrm{num}} \right) l_i(-1), \quad i = 0, \dots, K, \tag{13}$$

arises. Here, f^{num} is a suitably chosen numerical flux. Numerical fluxes provide a mechanism to couple the solutions across elements and typically depend on the values left and right of the interface.

The last discretisation step is to evaluate the spatial integrals in the strong form (13) by a suitable quadrature rule. Still following the idea of collocation, the quadrature points are also matched with the interpolation points $\{\xi_k\}_{k=0}^K$, yielding high efficiency for the numerical scheme. The resulting method is typically called the strong formulation of the *Discontinuous Galerkin collocation spectral element method* (*DGSEM*), see for instance [4] and references therein.

For sake of simplicity, we will just focus on the Gauss-Lobatto points for the interpolation as well as quadrature points $\{\xi_j\}_{j=0}^K$ and denote the associated integration weights by $\{\omega_j\}_{j=0}^K$. The analytic integration is replaced by the resulting quadrature rule

$$\int_{-1}^{1} g(\xi) \, \mathrm{d}\, \xi \approx \sum_{j=0}^{K} \omega_j g(\xi_j) \tag{14}$$

then. Besides the Gauss-Lobatto points, the Gauss-Legendre points are another typical choice for the collocation approach, which result in some different properties. See for instance the works [3,16] of Kopriva and Gassner.

By utilising the mass, differentiation, stiffness, boundary integral, and restriction (interpolation) matrices

$$\underline{\underline{M}} = \operatorname{diag}\left([\omega_0, \dots, \omega_K]\right), \qquad \underline{\underline{D}}_{jk} = l_k'(\xi_j), \qquad \underline{\underline{S}}_{ik} = \int_{-1}^{1} l_i l_k' \,\mathrm{d}\,\xi \quad \text{with} \quad \underline{\underline{S}} = \underline{\underline{M}}\,\underline{\underline{D}}, \tag{15}$$

$$\underline{\underline{B}} = \begin{pmatrix} -1 & 0 \\ 0 & 1 \end{pmatrix}, \qquad \underline{\underline{R}} = \begin{pmatrix} l_0(-1) & \dots & l_K(-1) \\ l_0(1) & \dots & l_K(1) \end{pmatrix}, \tag{16}$$

the DGSEM semidiscretisation can be rewritten in its matrix form

$$\frac{\Delta x}{2}\underline{\underline{M}}\,\partial_t \underline{u} = -\underline{\underline{S}}\,\underline{f} - \underline{\underline{R}}^T\underline{\underline{B}}\left(\underline{f}^{\text{num}} - \underline{\underline{R}}\,\underline{f}\right). \tag{17}$$

Here, $\underline{u}, \underline{f}$ are vectors containing the nodal coefficients of u_K, f_K with respect to the Gauss-Lobatto interpolation polynomials, and $\underline{f}^{\text{num}} = (f_L^{\text{num}}, f_R^{\text{num}})^T$ is the vector containing the values of the numerical flux at the element boundaries. Note that (17) essentially is a direct approximation of the conservation law on the left hand side augmented by a flux penalty term on the right hand side.

The resulting system of ordinary differential equations

$$\dot{\underline{u}} = L(\underline{u}) \tag{18}$$

for the solution coefficients $\underline{u}$, can be marched forward in time using, for instance, a Runge-Kutta method then. See the extensive literature [10–12, 15, 20]. In this work, all later numerical tests are obtained by the explicit strong stability preserving (SSP) Runge-Kutta (RK) method of third order using three stages (SSPRK(3,3)) given by Gottlieb and Shu in [11].

2.2. Typical drawbacks

High order DG methods are a commonly accepted and widely used semidiscretisation for hyperbolic conservation laws, advection-diffusion equations, and other models representing the behaviour of fluids. Yet, certain bottlenecks arise in their practical application. It will be these drawbacks that motivate the introduction of the DOP-LS approach in the DG framework in section 3 respectively section 4.

Among other works, in [8, 18], notably harsh time step restrictions have been pointed out for commonly used sets of collocation points. The authors argument essentially is that - by the well-known Courant-Friedrichs-Levy (CFL) condition - the time step has to be proportional to the spatial resolution for an explicit time step to be stable. More precise, the time step has to be proportional to the smallest distance between any two interpolation points $\{\xi_j\}$ in any element Ω_i. Denoting the smallest length among all elements by Δx, the CFL condition is given by

$$\Delta t \sim \Delta x \cdot \min_{j=1,\dots,K}\{\xi_j - \xi_{j-1}\}, \tag{19}$$

where the minimum occurs at the element boundaries for typical interpolation points such as the Gauss-Legendre and Gauss-Lobatto points. Using the asymptotic formula (22.16.6) in [1] for zeros of the Legendre polynomials as well as the small-angle approximation for $\cos\theta$, the smallest distance is proportional to K^{-2} for $K \to \infty$. Thus, the time step restriction

$$\Delta t \sim \Delta x \cdot K^{-2} \tag{20}$$

arises for the Gauss-Legendre points. A similar CFL condition also occurs for the Gauss-Lobatto points and other typical collocation points clustered at the boundaries. A way to overcome this problem is to use implicit time integration. Yet, the resulting ODE-system (18) typically is nonlinear. Even if linear, e.g. for the linear advection equation, the differentiation matrix $L = \underline{\underline{L}}$ often is dense. Since, implicit time marching algorithms are highly time consuming. As a solution, for instance Gelb, Platte, and Rosenthal aimed to construct a robust spectral method on equally distributed points by using DOP-LS approximations in [8], in order to advance explicitly in time with a less restrictive CFL condition. In fact, DOP-LS approximations

are able to provide high accuracy even on equidistant points, which are somewhat optimal from point of the CFL condition. It should be stressed, however, that their DOP-LS approximations were build on discrete weights corresponding to the class of super Gaussian weight functions. As it will be showcased later, such weights are unsuitable for the application in DG methods.

It is our opinion that further arguments for DOP-LS approximations should be brought into focus. DG methods, for instance, seriously lack in robustness. When formulated on equidistant points, as it was initially proposed by Reed and Hill in [23] on triangular elements, robustness as well as high orders (four and above) of accuracy are detained by the Runge phenomon. Also see the monograph [2] of Cockburn, Karniadakis, and Shu. In order to avoid the Runge phenomenon as well as to achieve highest orders of accuracy for both, interpolation and numerical integration, present-day DG methods are therefore constructed on Gauss-Legendre and Gauss-Lobatto like points. By the summation-by-parts property, these methods are further able to provide entropy stability for sufficiently smooth solutions, see for instance the works [4,5,17] of Kopriva, Gassner, and Winters. Extraordinary care has to be taken for the enforcement of boundary conditions, [21]. Even slight changes in the boundary conditions seem to render these methods to become unstable. Also minor perturbation of single nodal values yield significant changes in the resulting interpolation polynomial. Even though providing entropy stability, modern DG methods are still more or less unstable in practice. Further problems emerge in the presence of shock discontinuities.

3. Discrete orthogonal polynomial least squares approximations

While common DG methods, and in particular polynomial interpolation, lack in robustness, discrete least squares (DLS) approximations, hold promise to provide a much more stable alternative. By using more information of the underlying function, DLS approximations rely considerably less on single nodal values. Still maintaining high accuracy, robustness is even possible on equidistant points.

3.1. Discrete least squares approximations

The principle of discrete least squares is of primary computational interest. Originally, it was born from the wish to fit a linear mathematical model to given observations. In this work, we use the DLS principle to fit polynomials $u_{K,N}$ of degree K or less to observations given by nodal values at the collocation points. To reduce the influence of errors in the nodal values we proceed to use a greater number N of measurements than the number of $K+1$ unknown modal coefficients of the polynomial $u_{K,N}$. This results in the problem to 'solve' an overdetermined linear system of equations.

Given is a set of N observations $\underline{u}^{\text{obs}} = (u_1^{\text{obs}}, \dots, u_N^{\text{obs}})$ by nodal values $u_j^{\text{obs}} = u(\xi_j)$ at N collocation points $\{\xi_j\}_{j=1}^N$ in $[-1,1]$ and a basis $\{\varphi_k\}_{k=0}^K$ of $\mathbb{P}_K([-1,1])$. The higher level idea is to determine modal coefficients $\hat{u}_{k,N}$ such that the resulting polynomial

$$\sum_{k=0}^{K} \hat{u}_{k,N} \varphi_k(\xi) \tag{21}$$

fits the observations u_j^{obs} at the collocation points ξ_j, $j = 1, \dots, N$. By further denoting the matrix which contains the values of the basis function φ_k at the collocation points by

$$\underline{\underline{A}} = \big(\varphi_{k-1}(\xi_j)\big)_{k,j=1}^{K+1,N}, \tag{22}$$

the problem is to find a vector of modal coefficients $\underline{\hat{u}} = \big(\hat{u}_{0,N}, \dots, \hat{u}_{K,N}\big)$ such that $\underline{\underline{A}}\,\underline{\hat{u}}$ is the 'best' approximation to $\underline{u}^{\text{obs}}$. Referring to $\underline{r} = \underline{\underline{A}}\,\underline{\hat{u}} - \underline{u}^{\text{obs}}$ as the *residual vector*, the problem can likewise be stated as to 'minimise' the residual vector $\underline{r}$.

In fact, there are many possible ways of defining the 'best' approximation, respectively the 'minimal'

residual vector. In 1799, Laplace used the principle of minimising the sum of the absolute residual errors

$$\sum_{j=1}^{N} |r_j| \tag{23}$$

with the additional condition that the sum of the residual errors should be equal to zero, [9]. He then concluded that such a solution must satisfy exactly $K+1$ out of the N equations. In response to Laplace' results, Gauss opposed that such a solution, satisfying exactly $K+1$ equations, has to be regarded inconsistent with the laws of probability, since smaller or greater errors should be equally possible in all equations. Inspired by this idea, Gauss consequently went out to formulate the *principle of least squares*, where now the sum of squared residual errors

$$\sum_{j=1}^{N} r_j^2 \tag{24}$$

is minimised. First famous examples for the least squares method include the analysis of survey data and astronomical calculations, such as the successfully predicted orbit of the asteroid *Ceres* by Gauss in 1801, [6].

In this work, we utilise the further generalised principle of *weighted least squares*, where the residual vector is minimised in a weighted discrete l^1 norm

$$\|\underline{r}\|_\omega^2 = \sum_{j=1}^{N} \omega_j r_j^2. \tag{25}$$

The resulting problem of *discrete least squares* (DLS) can thus be formulated as

$$\min_{\underline{\hat{u}}} \left\| \underline{\underline{A}}\, \underline{\hat{u}} - \underline{u}^{\mathrm{obs}} \right\|_\omega . \tag{26}$$

In the fields of data fitting and signal processing, the weights $\omega_j \geq 0$, $j = 1, \ldots, N$, are typically utilised to control the influence of an observation u_k^{obs} on the fitting procedure, see [24]. Weights are chosen proportional to the probability that the corresponding observation is correct. In our novel DG method using the principle of DLS, however, the weights are determined by quadrature rules for numerical integration.

3.2. Discrete orthogonal polynomials

In order to reasonably work the DLS principle into the framework of DG methods, an efficient algorithm is needed to compute the modal coefficients $\underline{\hat{u}}$ which minimise (25). To the polynomial $u_{K,N}$ associated to the DLS vector of modal coefficients $\underline{\hat{u}}$ corresponding to the nodal observations $\underline{u}^{\mathrm{obs}}$ of an underlying function u, i.e.

$$u_{K,N}(\xi) = \sum_{k=0}^{K} \hat{u}_{k,N} \varphi_k(\xi), \tag{27}$$

we refer to as the *discrete least squares approximation*. This polynomial is further characterised by the relation

$$\left\| u - u_{K,N} \right\|_\omega = \min_{v \in \mathbb{P}_K} \|u - v\|_\omega , \tag{28}$$

or equivalently

$$\left\langle u - u_{K,N},\, v \right\rangle_\omega = 0 \quad \forall v \in \mathbb{P}_K, \tag{29}$$

where $\langle f,\, g\rangle_\omega := \sum_{j=1}^N \omega_j f(\xi_j) g(\xi_j)$ is the associated inner product. Since the DLS approximations $u_{K,N}$ can be expressed by (27) in a basis $\{\varphi_k\}_{k=0}^K$, relation (29) yields the linear $(K+1)\times(K+1)$ system of equations

$$\sum_{k=0}^{K} \hat{u}_{k,N} \langle \varphi_k,\, \varphi_i\rangle = \langle u,\, \varphi_i\rangle\,, \quad i = 0,\dots,K, \tag{30}$$

which can for instance be solved by Gaussian elimination.

Similar to modal bases in DG methods, highest efficiency is obtained by choosing the basis $\{\varphi_k\}_{k=0}^K$ to be orthogonal with respect to the underlying inner product, i.e.

$$\langle \varphi_k,\, \varphi_i\rangle_\omega = \delta_{ki} \|\varphi_k\|_\omega^2\,. \tag{31}$$

Then, the sum in (30) reduces to a single entry and the coefficients are given by

$$\hat{u}_{k,N} = \frac{\langle u,\, \varphi_k\rangle_\omega}{\|\varphi_k\|_\omega^2} \tag{32}$$

for $k = 0,\dots,K$. Orthogonal bases of polynomials $\{\varphi_k\}_{k=0}^K$ with respect to a discrete inner product are usually called *discrete orthogonal polynomials* (DOP) and the discrete least squares approximation $u_{K,N}$ is therefore also referred to as the *discrete orthogonal polynomial least squares* (DOP-LS) approximation.

Note that once we have decided for a discrete inner product, i.e. certain collocation points $\{\xi_j\}_{j=1}^N$ and weights $\{\omega_j\}_{j=1}^N$, there are basically two steps in order to compute the DOP-LS approximation $u_{K,N}$:

1. Find a basis of discrete orthogonal polynomials $\{\varphi_k\}_{k=0}^K$.
2. Compute the modal coefficients $\hat{u}_{k,N}$ by simply evaluating finite sums.

In general, the first step is obviously dodgier than the second. For non-classical orthogonal polynomials, often no explicit formula is known for the orthogonal polynomials $\{\varphi_k\}_{k=0}^K$.

Thus, recursive procedures, such as the Stieltjes procedure, see [7], or Gram-Schmidt like algorithms have to be applied. Beginning with $\varphi_{-1} = 0, \varphi_0 = 1$, all further basis elements can be built up successively by the three-term recurrence relation

$$\varphi_{k+1}(\xi) = (\xi - \alpha_k)\,\varphi_k(\xi) - \beta_k \varphi_{k-1}(\xi), \tag{33}$$

for $k = 0,\dots,K-1$. The recursion coefficients are given by

$$\alpha_k = \frac{\langle \xi\varphi_k,\, \varphi_k\rangle_\omega}{\langle \varphi_k,\, \varphi_k\rangle_\omega}, \qquad \beta_k = \frac{\langle \varphi_k,\, \varphi_k\rangle_\omega}{\langle \varphi_{k-1},\, \varphi_{k-1}\rangle_\omega}, \tag{34}$$

and can be computed in tandem with the discrete orthogonal polynomial φ_k.

Note that for symmetric weights, i.e. weights $\{\omega_j\}_{j=1}^N$ lying on a symmetric point distribution $\{\xi_j\}_{j=1}^N$ such that

$$\omega_j = \omega_{N+1-j}, \quad \text{for} \quad j = 1,\dots,N, \tag{35}$$

all recursion coefficients α_k vanish since $\xi\varphi_k^2$ is an odd function. Thus, in the case of symmetric weights, the Stieltjes recurrence relation (33) reduces to a more simple recurrence relation,

$$\begin{aligned} \varphi_0(\xi) &= 1, \quad \varphi_1(\xi) = \xi, \\ \varphi_{k+1}(\xi) &= \xi\varphi_k(\xi) - \frac{h_k}{h_{k-1}}\varphi_{k-1}(\xi), \quad \text{where} \quad h_k = \|\varphi_k\|_\omega^2 = \langle \varphi_k,\, \varphi_k\rangle_\omega\,, \end{aligned} \tag{36}$$

for symmetric weights.

Remark 3.1. It should be stressed that several disadvantages arise when implementing iterative approaches like the one above. Classical inner products (integrals), such as the L^2 inner product, are often computed numerically. When computing the norms h_k by a quadrature rule, however, for non-classical orthogonal polynomials[1] numerical errors arise which might get worse due to error propagation in iterative algorithms. This problem is overcome by using discrete orthogonal polynomials, since the h_k's are exactly evaluated as simple finite sums (except for round-off errors) then.

4. A novel DG method using DOP-LS approximations

In this section, a novel DG method is proposed using DOP-LS approximations. DG methods are essentially constructed by the idea to approximate u and f by certain polynomials u_K, f_K and to force the corresponding residual $\mathcal{R}_K = \partial_t u_K + \partial_x f_K$ to vanish in the sense that it should be orthogonal to a certain set of test functions subsequently. In section 2, the DGSEM was in particular constructed by polynomial interpolations u_K, f_K and the idea of collocation. Here, we propose the idea of using DOP-LS approximations $u_{K,N}, f_{K,N}$ as well as to replace integrals by discrete counterparts, i.e. sums. Again, the idea of collocation will be utilised, i.e. all collocation points are the same. The resulting novel DG method, will be referred to as the *discontinuous Galerkin discrete least squares (DG-DLS) method*. In subsection 4.1, a modal formulation using the modal coefficients of the DOP-LS approximations $u_{K,N}, f_{K,N}$ with respect to the basis of discrete orthogonal polynomials will be given. Second, a nodal reformulation using the nodal values of $u_{M,N}$ at the collocation points, i.e. the observations $u_j^{\text{obs}} = u(\xi_j)$, is derived in section 4.2. Both representations have their own advantages.

4.1. Modal formulation

Following the description of section 2, we again consider a scalar conservation law in one space dimension. Mapping each element to the reference element $\Omega_{ref} = [-1, 1]$ by transformation (4), the original equation is transformed into the reference space,

$$\frac{\Delta x}{2}\partial_t u + \partial_\xi f(u) = 0, \tag{37}$$

where all computations are performed. Yet, instead of a polynomial interpolation, we propose to approximate u by a DOP-LS approximation $u_{K,N}$ of order K and with respect to $N \geq N+1$ weights $\{\omega_j\}_{j=1}^N$ at collocation points $\{\xi_j\}_{j=1}^N$ in $[-1, 1]$. Using more information of the underlying function, the DLS approximations rely considerably less on single nodal values than, for instance, the polynomial interpolation, and thus holds promise to provide a much more stable alternative. When further utilising a basis of DOPs $\{\varphi_k\}_{k=0}^K$ associated to the weights $\{\omega_j\}_{j=1}^N$, the DOP-LS approximation on an element Ω_i is given by orthogonal projection,

$$u(t,x)\big|_{\Omega_i} \approx u_{K,N}(t,\xi) = \sum_{k=0}^{K} \hat{u}_{k,N}(t)\varphi_k(\xi), \tag{38}$$

where $\hat{u}_{k,N}(t)$ are the time depended modal coefficients given by (32), i.e.

$$\hat{u}_{k,N} = \frac{1}{h_k}\langle u,\, \varphi_k\rangle_\omega = \frac{1}{h_k}\sum_{j=1}^{N} \omega_j u(\xi_j)\varphi_k(\xi_j), \quad h_k = \|\varphi_k\|_\omega^2 . \tag{39}$$

In the same manner, we approximate the flux f by

$$f(u)\big|_{\Omega_i} \approx f_{K,N}(t,\xi) = \sum_{k=0}^{K} \hat{f}_{k,N}(t)\varphi_k(\xi) \quad \text{with} \quad \hat{f}_{k,N} = \frac{1}{h_k}\langle f,\, \varphi_k\rangle_\omega = \frac{1}{h_k}\sum_{j=1}^{N} \omega_j f(u(\xi_j))\varphi_k(\xi_j). \tag{40}$$

[1] for which no explicit formula is known

Inserting both DOP-LS approximations into the transformed equation (37), we obtain

$$\frac{\Delta x}{2}\partial_t u_{K,N}(t,\xi) + \partial_\xi f_{K,N}(t,\xi) = 0 \tag{41}$$

on the reference element Ω_{ref}. Now multiplying by a DOP basis function $\varphi_i \in \{\varphi_k\}_{k=0}^K$, integrating over the reference element, and applying integration by parts twice, the locally defined strong form,

$$\int_{-1}^{1} \left(\frac{\Delta x}{2}\partial_t u_{K,N} + \partial_\xi f_{K,N} \right) \varphi_i \,\mathrm{d}\,\xi = \left(f_{K,N}(1) - f_R^{\text{num}} \right) \varphi_i(1) - \left(f_{K,N}(-1) - f_L^{\text{num}} \right) \varphi_i(-1), \tag{42}$$

for $i = 0, \ldots, K$, arises. Again, f^{num} is a suitably chosen numerical flux. The last discretisation step in our DG-DLS method is to replace the continuous inner products (integrals) in (42) by discrete ones (sums) as well, i.e.

$$\int_{-1}^{1} \varphi_k(\xi)\varphi_i(\xi) \,\mathrm{d}\,\xi \quad \mapsto \quad \langle \varphi_k,\, \varphi_i \rangle_\omega = \sum_{j=1}^{N} \omega_j \varphi_k(\xi_j)\varphi_i(\xi_j). \tag{43}$$

To the resulting discretisation,

$$\left\langle \mathcal{R}_{K,N},\, \varphi_i \right\rangle = \left(f_{K,N}(1) - f_R^{\text{num}} \right) \varphi_i(1) - \left(f_{K,N}(-1) - f_L^{\text{num}} \right) \varphi_i(-1), \quad \forall \varphi \in \{\varphi_k\}_{k=0}^K, \tag{44}$$

with residual $\mathcal{R}_{K,N} = \frac{\Delta x}{2}\partial_t u_{K,N} + \partial_\xi f_{K,N}$, we will refer to as the *discontinuous Galerkin discrete least squares (DG-DLS) method*.

For the new DG-DLS method, a matrix representation can be formulated once more. By using the *mass* and *stiffness matrices*

$$\underline{\underline{M}} = \left(\langle \varphi_i,\, \varphi_k \rangle_\omega \right)_{i,k=0}^K = \operatorname{diag}\left([h_0, \ldots, h_K] \right), \qquad \underline{\underline{S}} = \left(\left\langle \varphi_i,\, \varphi_k' \right\rangle_\omega \right)_{i,k=0}^K \tag{45}$$

as well as the *boundary integral* and *restriction matrices*

$$\underline{\underline{B}} = \begin{pmatrix} -1 & 0 \\ 0 & 1 \end{pmatrix}, \qquad \underline{\underline{R}} = \begin{pmatrix} \varphi_0(-1) & \ldots & \varphi_K(-1) \\ \varphi_0(1) & \ldots & \varphi_K(1) \end{pmatrix}, \tag{46}$$

all with respect to the DOP basis $\{\varphi_k\}_{k=0}^K$, the matrix form of the *modal DG-DLS* method is given by

$$\frac{\Delta x}{2}\underline{\underline{M}}\,\partial_t \underline{\hat{u}} = -\underline{\underline{S}}\,\underline{\hat{f}} - \underline{\underline{R}}^T \underline{\underline{B}} \left(\underline{f}^{\text{num}} - \underline{\underline{R}}\,\underline{\hat{f}} \right). \tag{47}$$

Here, $\underline{\hat{u}}, \underline{\hat{f}}$ are the vectors containing the modal coefficients of $u_{K,N}, f_{K,N}$ with respect to the DOP basis $\{\varphi_k\}_{k=0}^K$, and $\underline{f}^{\text{num}} = (f_L^{\text{num}}, f_R^{\text{num}})^T$ again is the vector containing the values of the numerical flux at the element boundaries.

Note that there are different options to compute the mass and stiffness matrices. By using the *weight*, *Vandermonde*, and *differentiation matrices*

$$\underline{\underline{W}} = \operatorname{diag}\left([\omega_1, \ldots, \omega_N] \right), \quad \underline{\underline{V}} = \left(\varphi_{i-1}(\xi_j) \right)_{j,i=1}^{N,K+1}, \quad \underline{\underline{D}} = \left(\varphi_{k-1}'(\xi_j) \right)_{j,k=1}^{N,K+1}, \tag{48}$$

the mass and stiffness matrix can be rewritten as

$$\underline{\underline{M}} = \underline{\underline{V}}^T \underline{\underline{W}}\,\underline{\underline{V}} \qquad \text{respectively} \qquad \underline{\underline{S}} = \underline{\underline{V}}^T \underline{\underline{W}}\,\underline{\underline{D}}. \tag{49}$$

We think this is more practical from point of implementation, since $\underline{\underline{V}}$ and $\underline{\underline{D}}$ can be both computed simply by utilising the Stieltjes recurrence relation (36). Also the restriction matrix $\underline{\underline{R}}$ is simply derived from the Vandermonde matrix $\underline{\underline{V}}$.

In our implementation, however, we compute the stiffness matrix by the relation

$$\underline{\underline{S}} = \underline{\underline{M}}\,\underline{\underline{\hat{D}}}, \tag{50}$$

where the (modal) differentiation matrix $\underline{\underline{\hat{D}}}$ is the matrix representation of the linear differentiation operator on $\mathbb{P}_K$ with respect to the DOP basis $\{\varphi_k\}_{k=0}^K$. A recursively defined representation for $\underline{\underline{\hat{D}}}$ can be derived from the Stieltjes recurrence relation (36) and is provided in the appendix.

4.2. Nodal formulation

Note that for an non-linear flux f, the modal DOP-LS coefficients $\underline{\hat{f}} \in \mathbb{R}^{K+1}$ are computed using the nodal values $\underline{f} \in \mathbb{R}^N$ at the collocation points. The nodal values $\underline{f}$ are in turn computed by using the nodal values $\underline{u}$ which have to be extrapolated from the modal DOP-LS coefficients $\underline{\hat{u}}$. In summary, we have to translate between modal and nodal coefficients in every time step. To bypass this procedure, we propose an alternative nodal reformulation of the DG-DLS method in this subsection. All computations will then be performed solely with respect to the nodal coefficients $\underline{u}$ and $\underline{f}$.

Since

$$u_{K,N}(\xi) = \sum_{k=0}^{K} \hat{u}_{k,N}\varphi_k(\xi), \quad \hat{u}_{k,N} = \frac{1}{h_k}\sum_{j=1}^{N} \omega_j u(\xi_j)\varphi_k(\xi_j), \tag{51}$$

the DOP-LS approximation can also be calculated directly from the discrete data $u(\xi_j)$ as

$$u_{K,N}(\xi) = \sum_{k=0}^{K}\left(\frac{1}{h_k}\sum_{j=1}^{N}\omega_j u(\xi_j)\varphi_k(\xi_j)\right)\varphi_k(\xi) = \sum_{j=1}^{N} u(\xi_j)\underbrace{\left(\omega_j\sum_{k=0}^{K}\frac{\varphi_k(\xi_j)\varphi_k(\xi)}{h_k}\right)}_{=:g_j(\xi)}. \tag{52}$$

Thus, the derivative of the DOP-LS approximation can as well be written as

$$u'_{K,N}(\xi) = \sum_{j=1}^{N} u(\xi_j) g'_j(\xi) \quad \text{with} \quad g'_j(\xi) = \omega_j \sum_{k=0}^{K}\frac{\varphi_k(\xi_j)\varphi'_k(\xi)}{h_k}. \tag{53}$$

This time multiplying the DOP-LS residual (41) by a nodal function $g_i \in \{g_j\}_{j=1}^N$, yet again integrating over the reference element and applying integration by parts twice, the locally defined strong form,

$$\int_{-1}^{1}\left(\frac{\Delta x}{2}\partial_t u_{K,N} + \partial_\xi f_{K,N}\right) g_i \,\mathrm{d}\,\xi = \left(f_{K,N}(1) - f_R^{\text{num}}\right) g_i(1) - \left(f_{K,N}(-1) - f_L^{\text{num}}\right) g_i(-1), \tag{54}$$

for $i = 1, \ldots, N$, arises. Once more, the DG-DLS method is obtained by finally replacing the continuous inner products (integrals) by a discrete one (sums).

Also for the *nodal DG-DLS* method, a matrix form is formulated. This time, by using the corresponding *mass* and *stiffness matrices*

$$\underline{\underline{\tilde{M}}} = \left(\langle g_i, g_k\rangle_\omega\right)_{i,k=1}^{N}, \qquad \underline{\underline{\tilde{S}}} = \left(\langle g_i, g'_k\rangle_\omega\right)_{i,k=1}^{N} \tag{55}$$

as well as the *boundary integral* and *restriction matrices*

$$\underline{\underline{B}} = \begin{pmatrix} -1 & 0 \\ 0 & 1 \end{pmatrix}, \qquad \underline{\underline{\tilde{R}}} = \begin{pmatrix} g_1(-1) & \ldots & g_N(-1) \\ g_1(1) & \ldots & g_N(1) \end{pmatrix} \tag{56}$$

with respect to the functions $\{g_j\}_{j=1}^N$, the matrix form of the nodal DG-DLS method is given by

$$\frac{\Delta x}{2}\underline{\underline{\tilde{M}}}\,\partial_t \underline{u} = -\underline{\underline{\tilde{S}}}\,\underline{f} - \underline{\underline{\tilde{R}}}^T\underline{\underline{B}}\left(\underline{f}^{\text{num}} - \underline{\underline{\tilde{R}}}\,\underline{f}\right). \tag{57}$$

Here, $\underline{u}, \underline{f}$ are vectors containing observations $u_j^{\text{obs}} = u(\xi_j), f(u_j^{\text{obs}})$ at the collocation points $\{\xi_j\}_{j=1}^N$, and $\underline{f}^{\text{num}} = (f_L^{\text{num}}, f_R^{\text{num}})^T$ again is the vector containing the values of the numerical flux at the element boundaries.

5. Conservation, linear stability, and construction of suitable weights

We wish for numerical solution $u_{K,N}$ given by the DG-DLS method to mimic certain properties of the exact solution. In particular, numerical solutions to conservation laws, $\partial_t u + \partial_x f(u) = 0$, are derived in order to preserve certain quantities. Assuming an exact solution u, *conservation*

$$\frac{\mathrm{d}}{\mathrm{d}t}\int_\Omega u(t,x)\,\mathrm{d}\,x = -f(u)\big|_{\partial\Omega} \tag{58}$$

is supposed to hold. This property is also fulfilled by the numerical solution $u_{K,N}$, when

$$\frac{\Delta x}{2}\int_{-1}^{1}\partial_t u_{K,N}(t,\xi)\,\mathrm{d}\,\xi = -\left(f_R^{\mathrm{num}} - f_L^{\mathrm{num}}\right) \tag{59}$$

holds on the reference element.

Another important design criterion for numerical schemes for hyperbolic conservation laws is *stability* and in particular *linear stability*. Assuming an exact (entropy) solution of the scalar hyperbolic conservation law $\partial_t u = \partial_x f(u) = 0$ with convex flux function f and periodic boundary conditions, the L^2 norm of the solution is supposed not to increase over time, i.e.

$$\frac{\mathrm{d}}{\mathrm{d}t}\|u\|_{L^2}^2 \leq 0. \tag{60}$$

Linear stability now refers to the property of a numerical scheme to mimic this behaviour in the fundamental case of the linear advection equation

$$\partial_t u + \partial_x u = 0, \tag{61}$$

i.e. $f(u) = u$. By noting that

$$\frac{\mathrm{d}}{\mathrm{d}t}\|u\|_{L^2}^2 = 2\int_\Omega \big(\partial_t u(t,x)\big)\,u(t,x)\,\mathrm{d}\,x \tag{62}$$

it is sufficient to show

$$\Delta x\int_{-1}^{1}\big(\partial_t u_{K,N}(t,\xi)\big)\,u_{K,N}(t,\xi)\,\mathrm{d}\,\xi \leq 0 \tag{63}$$

for the numerical DG-DLS solution $u_{K,N}$ on the reference element. Linear stability follows by summing up over all elements then.

Note that for both, conservation as well as linear stability, integrals have to be evaluated for polynomials of certain degrees, i.e.

$$\int_{-1}^{1} v(\xi)\,\mathrm{d}\,\xi \tag{64}$$

with $\deg v = K$ for conservation and $\deg v = 2K$ for linear stability. Given a set collocation points $\{\xi_j\}_{j=1}^N$ in $[-1,1]$, we thus need to choose the weights $\{\omega_j\}_{j=1}^N$ such that the discrete inner product $\langle\cdot,\,\cdot\rangle_\omega$ provides an quadrature rule

$$Q_\omega[v] := \langle v,\,1\rangle_\omega = \sum_{j=1}^{N}\omega_j v(\xi_j) \tag{65}$$

of sufficiently high order of exactness. More precise, the associated quadrature rule Q_ω has to exactly integrate all polynomials up to degree $d = K$ for conservation, respectively $d = 2K$ for linear stability. Denoting the exact integral of a function v by

$$I[v] := \int_{-1}^{1} v(\xi)\,\mathrm{d}\,\xi, \tag{66}$$

the quadrature rule is required to fulfil the *exactness condition*

$$Q_\omega[v] = I[v] \quad \forall v \in \mathbb{P}_d([-1,1]). \tag{67}$$

In subsection 5.1, we thus construct suitable weights on a sufficiently large number of given collocation points $\{\xi_j\}_{j=1}^N$. Choosing the 'right' weights will be the key to subsequently proof conservation and linear stability of the resulting DG-DLS method in subsection 5.2. We would like to stress again that both properties are shown to hold on *any* sufficiently large set of collocation points once suitable weights are determined.

5.1. Construction of suitable weights

In this subsection, we aim to construct weights $\{\omega_j\}_{j=1}^N$ lying on a given set of quadrature points $\{\xi_j\}_{j=1}^N$ in $[-1,1]$ such that the exactness condition (67) holds.

Speaking more generally, we are interested in a quadrature rule that is exact on a finite-dimensional function space

$$V = span\{\psi_i\}_{i=0}^d, \tag{68}$$

where the ψ_i's are linearly independent. For a given set of quadrature points, we thus require the $d+1$ *exactness conditions*

$$Q_\omega[\psi_i] = I[\psi_i], \quad i = 0, \dots, d, \tag{69}$$

to be fulfilled. In general, quadrature rules are known to require $N = d+1$ quadrature points to do so. The corresponding weights can then be found by solving the linear system

$$\underline{\underline{A}}\,\underline{\omega} = \underline{b}, \tag{70}$$

where the matrix

$$\underline{\underline{A}} = \big(\psi_i(\xi_{j+1})\big)_{i,j=0}^{d,N-1} \tag{71}$$

contains the values of the basis function ψ_i at the quadrature points ξ_j and the right hand side vector

$$\underline{b} = \big(I[\psi_k]\big)_{k=0}^d \tag{72}$$

consists of the *moments*. A sufficient condition for a unique solution $\underline{\omega}$ and thus the associated quadrature rule is that the matrix $\underline{\underline{A}}$ is regular. This is for instance fulfilled in our case of polynomial basis functions, i.e. $V = \mathbb{P}_d([-1,1])$.

Once the weights are computed, for instance by Gaussian elimination, a corresponding DOP basis $\{\varphi_k\}_{k=0}^K$ is desired again for an efficient use of the discrete least squares principle, see section 3. Remember that the construction of these can be achieved by the Stieltjes procedure, either in general form (33) or more practical form (36) for symmetric weights. Obviously, the reccurence relation (36) is favoured and thus the question arises when the above procedure of constructing quadrature rules provides symmetric weights. In fact, weights defined by (70) are symmetric if the quadrature points $\{\xi_j\}_{j=1}^N$ are symmetrically distributed in $[-1,1]$. This is noted by

Lemma 5.1. *Let $N = d+1$, $\{\xi_j\}_{j=1}^N$ be a set of quadrature points in $[-1,1]$ and $\{\psi_i\}_{i=0}^d$ be a basis of $\mathbb{P}_d([-1,1])$. The weights $\{\omega_j\}_{j=1}^N$ defined by (70) are symmetric if the quadrature points $\{\xi_j\}_{j=1}^N$ are symmetrically distributed.*

Proof. Let $\{\xi_j\}_{j=1}^N$ be a set of quadrature points in $[-1,1]$ and $\{\psi_i\}_{i=0}^d$ be a basis of $\mathbb{P}_d([-1,1])$. By (70), the quadrature rule Q_ω with respect to the weights $\{\omega_j\}_{j=1}^N$ is exact for all polynomials of degree d or less, i.e.

$$Q_\omega[\psi] = I[\psi] \quad \forall \psi \in \mathbb{P}_d([-1,1]) \tag{73}$$

holds.

Assuming the weights $\{\omega_j\}_{j=1}^N$ to be non-symmetric, there is an index $i \in \{1,\dots,N\}$ such that $\omega_i \neq \omega_{N+1-i}$. We can find an odd polynomial ψ, i.e. $I[\psi] = 0$, of degree d or less then such that

$$Q_\omega[\psi] = \omega_i - \omega_{N+1-i} \neq 0. \tag{74}$$

The polynomial ψ is constructed by polynomial interpolation with respect to the data set

$$\big(\xi_j, \psi_j\big) = \begin{cases} \big(\xi_j, 0\big) & , \quad j \neq i, N+1-i, \\ \big(\xi_j, 1\big) & , \quad j = i, \\ \big(\xi_j, -1\big) & , \quad j = N+1-i, \end{cases} \tag{75}$$

and yields a contradiction to the exactness condition (73). □

Example 5.2. Typical examples for quadrature rules include the Gauss-Lobbato and Gauss-Legendre rule on their corresponding quadrature points as well as the Newton-Cotes rule on equidistant points. Since equidistant points provide a quite pertinent example for a basic set of collocation points for which the common DG method fails for higher order, it will be this case we demonstrate the performance of our new DG-DLS method for in section 6.

Finally, it should be stressed that positivity of the weights is not guaranteed by the above approach. For instance, the Newton-Cotes rule on equidistant points is known to have weights with mixed signs for $N \geq 9$, see [13]. As a consequence, the quadrature rule does not only become numerically unstable but also convergence might fail. Exceeding the scope of this work, improvement of our novel DG-DLS method by positive quadrature rules will be exhaustively discussed in a forthcoming work.

5.2. Conservation and linear stability

In this subsection, we use the precedent determined weights to prove conservation as well as linear stability for the resulting DG-DLS methods. Note that both properties hold on any sufficiently large set of collocation points, where at most $N = K+1$ points are needed for conservation to hold and at most $N = 2K+1$ for linear stability.

The DG-DLS method was essentially designed in order for the equation

$$\big\langle \mathcal{R}_{K,N},\, \psi \big\rangle_\omega = \big(f_L^{\text{num}} - f_{K,N}(-1)\big)\,\psi(-1) - \big(f_R^{\text{num}} - f_{K,N}(1)\big)\,\psi(1) \tag{76}$$

to hold for all polynomials ψ of degree K or less. By setting $\psi \equiv 1$, this reduces to

$$\sum_{j=1}^N \omega_j \left(\frac{\Delta x}{2} \partial_t u_{K,N}(t,\xi_j) + \partial_\xi f_{K,N}(t,\xi_j) \right) = \big(f_L^{\text{num}} - f_{K,N}(-1)\big) - \big(f_R^{\text{num}} - f_{K,N}(1)\big)\,. \tag{77}$$

In order to proof conservation of the DG-DLS method, we use the weights determined in the previous subsection 5.1. Choosing $N \geq K+1$ and the corresponding weights $\{\omega_j\}_{j=1}^N$ given by (70), the resulting discrete inner product induces a quadrature rule which is exact for polynomials of degree K or less. Therefore,

$$\begin{aligned} \frac{\Delta x}{2} \int_{-1}^1 \partial_t u_{K,N}(t,\xi)\,\mathrm{d}\,\xi &= \sum_{j=1}^N \omega_j \frac{\Delta x}{2} \partial_t u_{K,N}(t,\xi_j) \\ &= -\left(\sum_{j=1}^N \omega_j \partial_\xi f_{K,N}(t,\xi_j) \right) + \big(f_L^{\text{num}} - f_{K,N}(-1)\big) - \big(f_R^{\text{num}} - f_{K,N}(1)\big) \\ &= -\int_{-1}^1 \partial_\xi f_{K,N}(t,\xi)\,\mathrm{d}\,\xi + \big(f_L^{\text{num}} - f_{K,N}(-1)\big) - \big(f_R^{\text{num}} - f_{K,N}(1)\big) \\ &= -\left(f_R^{\text{num}} - f_L^{\text{num}}\right) \end{aligned} \tag{78}$$

follows from (77). By summing up over all elements, conservation of our new DG-DLS method is proven.

For linear stability, this time we choose $\psi = u_{K,N}$ in (76), yielding

$$\begin{aligned}\sum_{j=1}^{N} \omega_j \left(\frac{\Delta x}{2} \partial_t u_{K,N}(t,\xi_j) + \partial_\xi u_{K,N}(t,\xi_j) \right) u_{K,N}(t,\xi_j) \\ = \left(f_L^{\text{num}} - u_{K,N}(-1) \right) u_{K,N}(t,-1) - \left(f_R^{\text{num}} - u_{K,N}(1) \right) u_{K,N}(t,1),\end{aligned} \tag{79}$$

since $f_{K,N} = u_{K,N}$ for the linear advection equation. It should be stressed that this time integrals over polynomials of degree $2K$ or less need to be evaluated. Choosing $N \geq 2K+1$ and utilising the weights $\{\omega_j\}_{j=1}^N$ given by (70), the resulting discrete sum again is equals to the continuous integral. Hence,

$$\begin{aligned}\frac{\Delta x}{2} \int_{-1}^{1} \left(\partial_t u_{K,N}(t,\xi) \right) u_{K,N}(t,\xi) \, \mathrm{d}\, \xi \\ = - \int_{-1}^{1} \left(\partial_\xi u_{K,N}(t,\xi) \right) u_{K,N}(t,\xi) \, \mathrm{d}\, \xi \\ + \left(f_L^{\text{num}} - u_{K,N}(-1) \right) u_{K,N}(t,-1) - \left(f_R^{\text{num}} - u_{K,N}(t,1) \right) u_{K,N}(t,1)\end{aligned} \tag{80}$$

follows analogously to (78). At the same time, due to integration by parts,

$$\begin{aligned}\int_{-1}^{1} \left(\partial_\xi u_{K,N}(t,\xi) \right) u_{K,N}(t,\xi) \, \mathrm{d}\, \xi = u_{K,N}^2(t,\xi) \Big|_{\xi=-1}^{1} - \int_{-1}^{1} u_{K,N}(t,\xi) \left(\partial_\xi u_{K,N}(t,\xi) \right) \mathrm{d}\, \xi \\ \iff 2 \int_{-1}^{1} \left(\partial_\xi u_{K,N}(t,\xi) \right) u_{K,N}(t,\xi) \, \mathrm{d}\, \xi = u_{K,N}^2(t,\xi) \Big|_{\xi=-1}^{1}\end{aligned} \tag{81}$$

holds. Substituting (81) into (80), we obtain

$$\begin{aligned}\Delta x \int_{-1}^{1} \left(\partial_t u_{K,N}(t,\xi) \right) u_{K,N}(t,\xi) \, \mathrm{d}\, \xi \\ = -u_{K,N}(t,1)^2 + u_{K,N}(t,-1)^2 \\ + \left(f_L^{\text{num}} - u_{K,N}(-1) \right) u_{K,N}(t,-1) - \left(f_R^{\text{num}} - u_{K,N}(t,1) \right) u_{K,N}(t,1) \\ = u_{K,N}(t,1) \left[u_{K,N}(t,1) - 2 f_R^{\text{num}} \right] - u_{K,N}(t,-1) \left[u_{K,N}(t,-1) - 2 f_L^{\text{num}} \right].\end{aligned} \tag{82}$$

Assuming periodic boundary conditions, the global rate of change cuts down to a sum of local contributions

$$u_- \left[u_- - 2 f^{\text{num}} \right] - u_+ \left[u_+ - 2 f^{\text{num}} \right]. \tag{83}$$

Here, considering a border between two neighbouring elements, f^{num} denotes a common numerical flux, while u_- denotes the value $u_{K,N}(t,1)$ at the right boundary of the element to the left and u_+ analogously denotes the value $u_{K,N}(t,-1)$ at the left boundary of the element to the right. If we, for instance, choose a common upwind numerical flux

$$f^{\text{num}}(u_-, u_+) = \frac{u_+ + u_-}{2} - \alpha (u_+ - u_-), \tag{84}$$

linear stability follows from

$$u_- \left[u_- - 2 f^{\text{num}} \right] - u_+ \left[u_+ - 2 f^{\text{num}} \right] = -2\alpha (u_- - u_+)^2 \leq 0, \tag{85}$$

where $\alpha \geq 0$. Here, $\alpha = 0$ corresponds to the entropy conservative central numerical flux $f^{\text{num}}(u_-, u_+) = (u_+ + u_-)/2$, while $\alpha = 1/2$ corresponds to the entropy stable full upwind numerical flux $f^{\text{num}}(u_-, u_+) = u_-$.

Conservation and linear stability of our new DG-DLS method utilising the principle of discrete least squares are summarised in the following

Theorem 5.3. *Let $K \in \mathbb{N}$ and $\{\xi_j\}_{j=1}^N$ any set of collocation points on the reference element $\Omega_{ref} = [-1, 1]$. By utilising the weights $\{\omega_j\}_{j=1}^N$ determined by (70), the discontinuous Galerkin discrete least squares (DG-DLS) method (44) is conservative for $N \geq K + 1$ and linear stable for $N \geq 2K + 1$.*[2]

6. Numerical results

In this section, the previous theoretical results are testifyed by several numerical tests. These tests further highlight our new DG-DLS method to significantly outperform present-day (interpolation based) DG methods.

For the numerical tests, we mainly focus on equidistant points, since they provide a basic yet highly challenging example. Common DG methods are known to have special problems handling collocation points which are uniformly distributed.

Note that all tests are performed on the spatial domain $[0, 2]$ and that time integration is performed by the explicit strong stability preserving (SSP) Runge-Kutta (RK) method of third order using three stages (SSPRK(3,3)) given by Gottlieb and Shu in [11].

We start our numerical investigation in subsection 6.1 by a linear problem which, in accordance to Theorem 5.3, highlights conservation as well linear stability of our new DG-DLS method. At the same time, this example demonstrates common DG methods to perform quite poor on equidistant points. In subsection 6.2, we then aim for an error analysis of the DG-DLS method and for the common DG method. Both methods are compared and the new DG-DLS method is again highlighted to provide significantly higher orders of accuracy. We close this section by a non-linear Burgers' test case featuring a shock as well as a rarefaction wave in the analytic reference solution. While the DG-DLS method is able to provide a fairly good numerical approximation, common DG methods are demonstrated to fail formidably in this test case. We have not seen this test case anywhere else. Yet, it is our conjecture that most - if not all - collocation approaches for which points lie on both element boundaries fail for this test case. This is also demonstrated for the recent DGSEM on Gauss-Lobatto points, which is a heavily used method

6.1. Conservation and linear stability

In this subsection, we numerically investigate conservation as well as linear stability for our new DG-DLS method with respect to different choices for the number of equidistant collocation points. This is done for the linear advection equation $\partial_t u = \partial_x u = 0$ and a smooth initial condition

$$u_0(x) = \exp\left(-20(x-1)^2\right) \tag{86}$$

for time $t \in [0, 4]$. Further, in all tests for the linear advection equation, the (full) upwind numerical flux (84) corresponding to $\alpha = \frac{1}{2}$ and periodic boundary conditions are used. Figure 1 shows the numerical solutions for $I = 20$ elements, polynomial degree $K = 4$, and $N = K + 1 = 5$ (common DG) in Figure 1a as well as $N = K + 1 = 5$ (DG-DLS) in Figure 1b. Besides the numerical solution (straight blue line), both Figures also show the analytic reference solution (dashed red line).

Note that the numerical solution by the common DG method - corresponding to the parameter choice $N = K + 1$ in the more general class of DG-DLS methods - shows heavy oscillations which pollute the solution. We think these oscillations already emerge at $t = 0$, due to the Runge phenomenon, and increase over time. At the same time, the parameter choice $N = 2K + 1$ in the DG-DLS method provides a considerably better solution. It is not possible, with the naked eye, to distinguish between the numerical and reference solution anymore. It should also be stressed that the numerical solution for $N = K + 1 = 5$ was computed using 40 000 time steps, while just 1 000 were used for $N = 2K + 1 = 9$.

Figure 1c and 1d are furthermore illustrating the total mass $\int_0^2 u(t, x)\,\mathrm{d}\,x$ and energy $\left\|u(t, \cdot)\right\|_\omega^2$ of the corresponding numerical solution over time. Here, the constant C is chosen such that $\int_0^2 u(0, x)\,\mathrm{d}\,x + C =$

[2] when, for instance, a common upwind numerical flux (84) is chosen

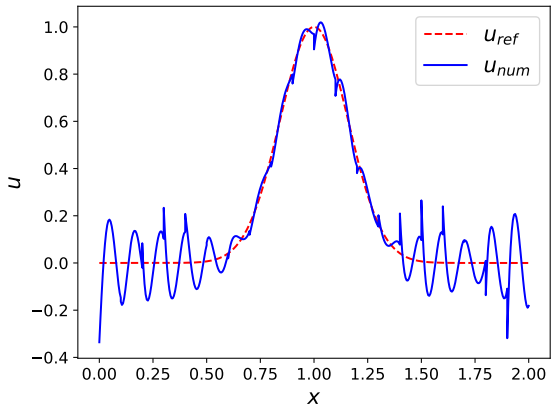

(a) Solution for $N = K + 1 = 5$ and 40000 time steps.

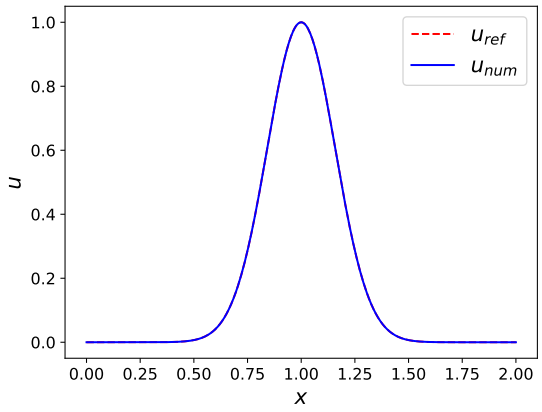

(b) Solution for $N = 2K + 1 = 9$ and 1000 time steps.

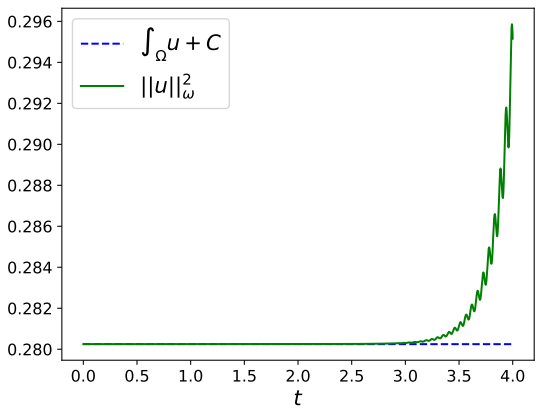

(c) Mass and energy for $N = 5$ and 40000 time steps.

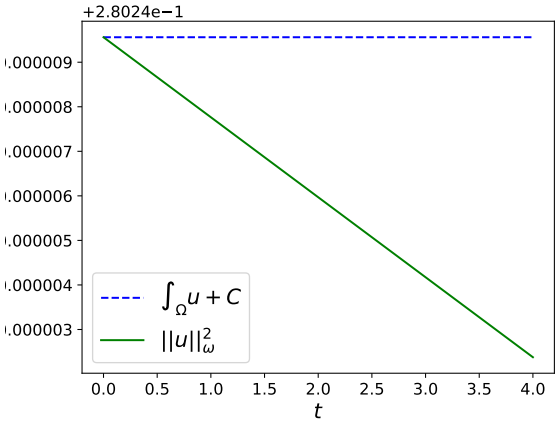

(d) Mass and energy for $N = 9$ and 1000 time steps.

Figure 1: Numerical solutions with their mass and energy for $K = 4$ by the DG-DLS method.

$\left\|u(0,\cdot)\right\|^2_\omega$. In accordance to Theorem 5.3, mass remains constant for both choices of N, while energy increases for $N = K + 1$ but slightly decreases for $N = 2K + 1$. As stated by Theorem 5.3 in particular, linear stability (not increasing energy) in general is just ensured for $N \geq 2K + 1$.

6.2. Error analysis and convergence

In this subsection an error and convergence analysis is given for our new DG-DLS method and the two parameter choices $N = K + 1$ and $N = 2K + 1$. Again, the linear advection equation $\partial_u + \partial_x u = 0$ with smooth initial condition (86) and periodic boundary conditions is considered on $\Omega = [0, 2]$. Yet, for the common DG method ($N = K + 1$) not to break down in the computations, we restrict the time to $t \in [0, 2]$ and use $100 \cdot I \cdot N$ time steps. The L^∞ errors for $N \in \{20, 40, 60, 80\}$ elements and polynomial degrees $K \in \{1, 2, 3, 4\}$ can be seen in Table 1a for $N = K + 1$ as well as in Table 1b for $N = 2K + 1$.

Note that the DG-DLS method for $N = 2K+1$ always - expect from the case $K = 1$ - provides significantly higher accuracy than the common DG method, i.e. for $N = K+1$. In fact, for $K = 4$ the Runge phenomenon seems to perform for the common DG approximation and thus pollutes the numerical solution, see the red marked values in Table 1a. Using the L^∞-errors, also the experimental order of convergence (EOC) with

I	K	L^∞-error	EOC(I)	EOC(K)
20	1	1.0719109786e-1		
20	2	1.1618825685e-2		3.21
20	3	8.0679316017e-4		6.58
20	4	1.5457899726e-4		5.74
40	1	2.2531359343e-2	2.25	
40	2	9.9199334956e-4	3.55	4.51
40	3	6.3943642589e-5	3.66	6.76
40	4	1.4388639567e-4	-	0.10
60	1	8.2924821538e-3	2.47	
60	2	2.3208096836e-4	3.58	5.16
60	3	1.3260091970e-5	3.88	7.06
60	4	8.2565289977e-4	-	-
80	1	4.0781711754e-3	2.47	
80	2	8.8716018393e-5	3.34	5.52
80	3	4.2543976567e-6	3.95	7.49
80	4	6.4437486562e-3	-	-

(a) Common DG method, $N = K + 1$.

I	K	L^∞-error	EOC(I)	EOC(K)
20	1	1.0799269819e-1		
20	2	4.0614959860e-3		4.73
20	3	2.5095142948e-4		6.87
20	4	1.6054263285e-5		9.56
40	1	2.2579118203e-2	2.26	
40	2	4.1542964992e-4	3.29	5.76
40	3	1.7425375380e-5	3.85	7.82
40	4	5.8790185741e-7	4.77	11.78
60	1	8.3017236178e-3	2.47	
60	2	1.1375701044e-4	3.19	6.19
60	3	3.4851992291e-6	3.97	8.60
60	4	7.9092124405e-8	4.95	13.16
80	1	4.0810762832e-3	2.47	
80	2	4.6609924479e-5	3.10	6.45
80	3	1.1079775560e-6	3.98	9.22
80	4	1.9063868483e-8	4.95	14.12

(b) Novel DG-DLS, $N = 2K + 1$.

Table 1: L^∞-errors and experimental orders of convergence (EOC) for the DG as well as DG-DLS method.

respect to an increasing number of elements I and polynomial degree K are provided in Table 1.[3] While both choices of parameters, $N = K + 1$ and $N = 2K + 1$, show a somewhat slow convergence in I, the new DG-DLS method demonstrates an outstandingly faster convergence in the polynomial degree K.

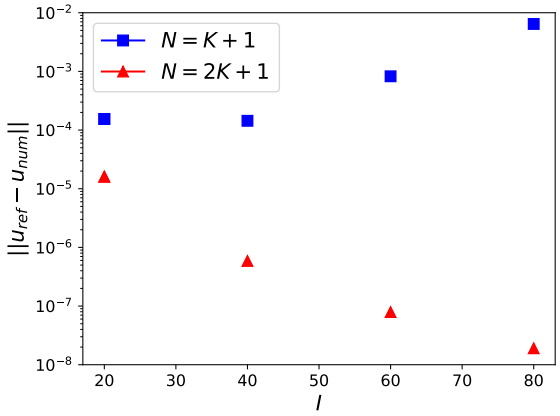

(a) Error for $K = 4$ and increasing I on a log scale.

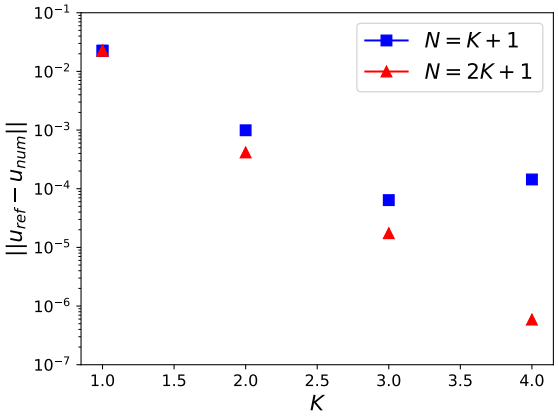

(b) Error for $I = 40$ and increasing K on a log scale.

Figure 2: L^∞ errors with respect to K and I.

Convergence for both choices of parameters is illustrated in Figure 2 on a logarithmic scale. Here, Figure 2a shows the convergence of the L^∞-errors for $K = 4$ and increasing number of elements $I = 20, 40, 60, 80$. Figure 2b, on the other hand, illustrates the convergence of the L^∞-errors for $I = 40$ and increasing polynomial degree $K = 1, 2, 3, 4$.

[3]- means that the order of convergence is not even positive

6.3. Shocks and rarefaction waves

In this last subsection, our new DG-DLS method is demonstrated for the non-linear example of Burgers' equation $\partial_t u + \partial_x \left(\frac{u^2}{2}\right) = 0$ on the spatial domain $\Omega = [0, 2]$ and for time $t \in [0, \frac{1}{2}]$. The initial condition is chosen as a square wave,

$$u_0(x) = \begin{cases} -1, & \text{for } x \leq 1 \text{ or } x \geq 1.5, \\ 1, & \text{for } 1 < x < 1.5, \end{cases} \tag{87}$$

and is known, by the method of characteristics, to yield a solution featuring both, a steady shock at $x = 1.5$ as well as a rarefaction wave around $x = 1$. The analytic reference solution (dashed red line) is illustrated in Figure 3 and Figure 4. The numerical solutions are all computed using $I = 81$ elements, polynomial degree $K = 3$ and 1 000 time steps. Again, periodic boundary conditions are used. For the numerical flux, the usual local Lax-Friedrichs flux

$$f^{\text{num}}(u_-, u_+) = \frac{1}{4}\left(u_+^2 + u_-^2\right) - \frac{\max\{|u_+|, |u_-|\}}{2}\left(u_+ - u_-\right), \tag{88}$$

is applied.

For this problem, the DG-DLS method is not only demonstrated for equidistant points but also for Gauss-Lobatto points. In the latter case, the parameter choice $N = K + 1$ corresponds to the discontinuous Galerkin collocation spectral element method (DGSEM) of Gassner and Kopriva [3,4,16]. Yet, the common DG methods fail for both choices of collocation points formidably. The numerical solution (straight blue line) for the DG-DLS method on equidistant points and the parameter choice $N = K + 1 = 4$, i.e. the common DG method, can be seen in Figure 3a. Figure 3b shows the corresponding numerical solution for $N = K + 1 = 7$.

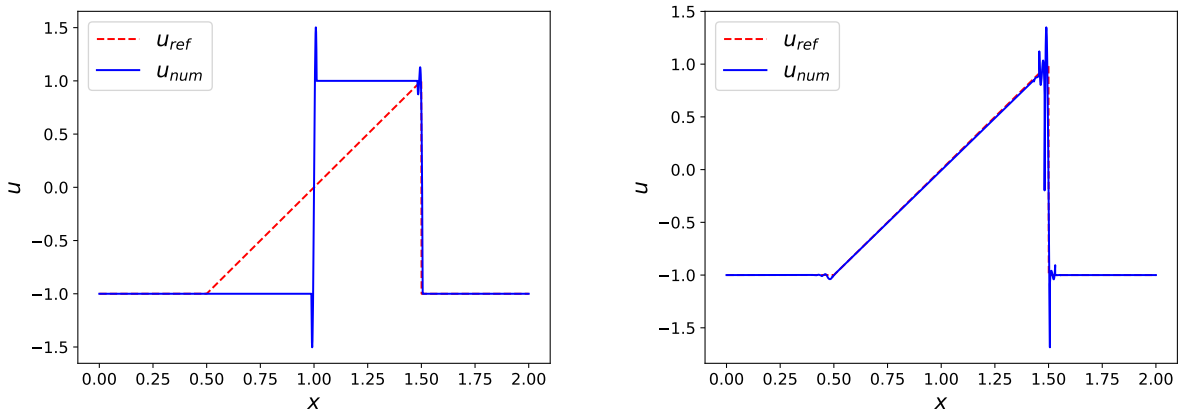

(a) Solution for $N = K + 1 = 4$ (common DG).

(b) Solution for $N = 2K + 1 = 7$ (DG-DLS).

Figure 3: Solutions by the DG-DLS method for $K = 3$ on equidistant points.

While the common DG method fails completely to capture the rarefaction wave in the reference solution, and thus provides a physically unreasonable solution, our new DG-DLS method with $N = 2K + 1$ provides a fairly good solution. Note that oscillations at $x = 1.5$ are unavoidable without post processing, due to the Gibbs phenomenon. We want to stress that the same observation can be made for the recently popular DGSEM on Gauss-Lobatto points, see Figure 4. Here, the DGSEM arises as a special case from our new DG-DLS method, when Gauss-Lobatto points are used and the parameter $N = K + 1$ is chosen. The corresponding numerical solution is shown by Figure 4a and again fails to provide a physically reasonable solution. At the same time, our DG-DLS method for $N = 2K + 1$ is able to do so in Figure 4b again.

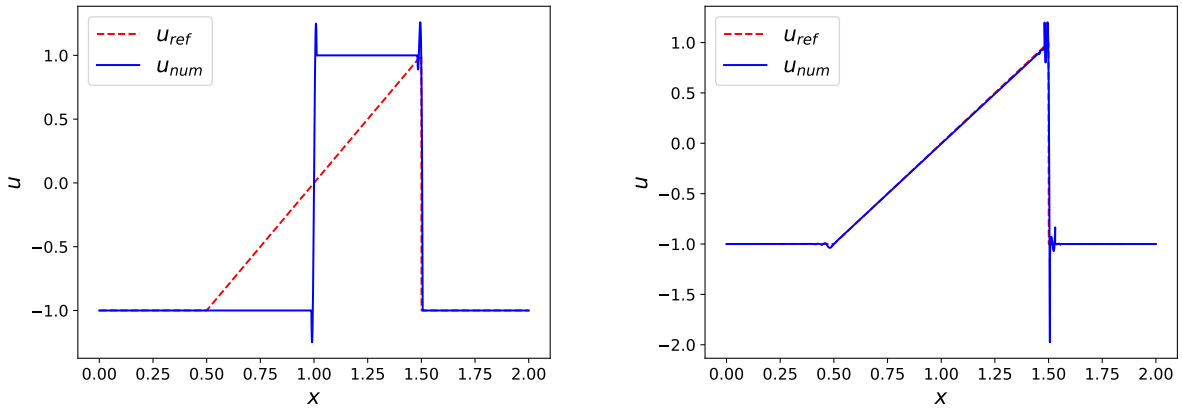

(a) Solution for $N = K + 1 = 4$ (common DGSEM).

(b) Solution for $N = 2K + 1 = 7$ (DG-DLS).

Figure 4: Solutions for $K = 3$ on Gauss-Lobatto points.

This is a serious shortcoming of most present-day DG methods. Even in this first non-linear test case of Burgers' equation they are not able to capture rarefaction waves, when the initial jump discontinuity lies in the interior of an element. The reason for this is that all nodal flux values are given by $f_j = f(u_j) = (\pm 1)^2 = 1$ and the resulting polynomial f_K thus becomes constant. By this argument, we conjecture that this phenomenon also arises for most other collocation methods, such as flux reconstruction, whenever points lie at the element boundaries. For common (interpolatory) collocation methods, this might just be overcome by collocation points not lying on the element boundaries, by skew-symmetric formulations of the differential equation, or by application of a sub-cell shock-capturing procedure, such as artificial viscosity or finite volume sub-cells. Also staggered grid approaches should avoid the phenomenon to occur. To the best of our knowledge, this test case and the resulting phenomenon was not discussed anywhere else yet.

Meanwhile, our new DG-DLS method is able to overcome this problem without any concerns.

7. Conclusion

In this work, a novel discontinuous Galerkin method was introduced by utilising the principle of discrete least squares. To the resulting class of new DG methods, which can be formulated on any set of collocation points, we referred to as *discontinuous Galerkin discrete least squares (DG-DLS)* methods. The key idea for our new method was to build the polynomial approximations $u_{K,N}, f_{K,N}$ by a weighted least squares approximation instead of interpolation or (discrete) L^2 projection. Our method thus utilises more information of the underlying function and provides a more robust alternative to common DG methods. As a result we were able to construct conservative as well as linear stable schemes on *any* set of collocation points whenever a sufficiently large number N of collocation points is used. This was summarised in our main result, Theorem 5.3. Care just has to be taken for the weights. These have to provide a quadrature rule with order of exactness K for conservation to hold and $2K$ for linear stability to further be ensured.

Several numerical tests highlighted our new DG-DLS method to significantly outperform present-day DG methods. The DG-DLS method is not only able to overcome instabilities related to the Runge phenomenon, but also to achieve formidable orders of accuracy. Finally, a test case for the Burgers' equation was proposed which shows common DG methods to fail to reproduce certain rarefaction waves. At the same, our new DG-DLS method is able to handle this test case and the resulting phenomenon without any concerns.

Finally, we would like to note distinguished recommendation for future research. Most obviously, applications of the new method to further models of conservation and balance laws, such as shallow water and Eulers' equations seem highly interesting. Before doing so, however, focus should be given to the incorpo-

ration of more stable quadrature rules. In particular the Newton-Cotes rule on equidistant points is known to feature weights with mixed signs for $N \geq 9$. As a consequence, the resulting quadrature rule does not only become numerically unstable, but also convergence is not ensured anymore. In a forthcoming work, we thus plan to further enhance the DG-DLS method by introducing stable high-order quadrature rules on arbitrary sets of collocation points.

Acknowledgement. This work developed during a two-month stay of the first author at the Max Planck Institute for Mathematics (MPIM) in Bonn during summer of 2017. He would like to express his gratitude for the generous financial support by the MPIM as well as the warm and inspiring research atmosphere provided by its staff.

A. Appendix

The elements $d_{i,k}$ of the differentiation matrix

$$\underline{\underline{\hat{D}}} = \left(d_{i,k}\right)_{i,k=0}^{K} \tag{89}$$

with respect to the DOP basis $\{\varphi_k\}_{k=0}^{K}$ are determined by the system of linear equations

$$\underline{\hat{u}'} = \underline{\underline{\hat{D}}}\,\underline{\hat{u}}, \qquad \text{respectively} \qquad \varphi_i' = \sum_{k=0}^{K} d_{i,k}\varphi_k, \quad i = 0, \dots, K, \tag{90}$$

where the vector $\underline{\hat{u}'}$ denotes the modal coefficients of the derivative of the polynomial u. Since $\{\varphi_k\}_{k=0}^{K}$ is an orthogonal basis with $\deg \varphi_k = k$, the equations reduce to

$$\varphi_i' = \sum_{k=0}^{i-1} d_{i,k}\varphi_k \tag{91}$$

for $i = 0, \dots, K$. By the Stieltjes recurrence relation (36), we have $\varphi_0 = 1, \varphi_1 = \xi$, and thus already

$$\varphi_0' = 0 \quad \Longrightarrow \quad d_{0,k} = 0 \quad \forall k = 0, \dots, K \tag{92}$$

$$\varphi_1' = 1 = \varphi_0 \quad \Longrightarrow \quad d_{1,0} = 1, \quad d_{1,k} = 0 \quad \forall k = 1, \dots, K. \tag{93}$$

In fact, $\underline{\underline{\hat{D}}}$ is a lower triangular matrix, since $d_{i,k} = 0$ holds for $k \geq i$ by (91).

Building on these first two rows of $\underline{\underline{\hat{D}}}$, we derive all other rows iteratively by going over to the derivative on both sides of the Stieltjes recurrence relation, i.e.

$$\varphi_{i+1}' = \varphi_i + \xi\varphi_i' - \tilde{h}_i\varphi_{i-1}' \tag{94}$$

for $i \geq 1$ and with $\tilde{h}_i = \frac{h_i}{h_{i-1}}$. By noting that

$$\xi\varphi_k = \varphi_{k+1} + \tilde{h}_k\varphi_{k-1}, \quad \text{for } k \geq 1, \tag{95}$$

we obtain

$$\begin{aligned}
\varphi_{i+1}' &= \varphi_i + \sum_{k=0}^{i-1} d_{i,k}\xi\varphi_k - \tilde{h}_i \sum_{k=0}^{i-2} d_{i-1,k}\varphi_k \\
&\overset{(95)}{=} \varphi_i + d_{i,0}\varphi_1 + \sum_{k=1}^{i-1} d_{i,k}\varphi_{k+1} + \sum_{k=1}^{i-1} \tilde{h}_k d_{i,k}\varphi_{k-1} - \tilde{h}_i \sum_{k=0}^{i-2} d_{i-1,k}\varphi_k \\
&= \varphi_i + d_{i,0}\varphi_1 + \sum_{k=2}^{i} d_{i,k-1}\varphi_k + \sum_{k=0}^{i-2} \tilde{h}_{k+1} d_{i,k+1}\varphi_k - \tilde{h}_i \sum_{k=0}^{i-2} d_{i-1,k}\varphi_k.
\end{aligned} \tag{96}$$

Summing up the coefficients, the elements in the $(i+1)$-th row of $\underline{\underline{\hat{D}}}$ are recursively defined by

$$\begin{aligned} d_{i+1,0} &= \tilde{h}_1 d_{i,1} - \tilde{h}_i d_{i-1,0}, \\ d_{i+1,1} &= d_{i,0} + \tilde{h}_2 d_{i,2} - \tilde{h}_i d_{i-1,1} \\ d_{i+1,k} &= d_{i,k-1} + \tilde{h}_{k+1} d_{i,k+1} - \tilde{h}_i d_{i-1,k}, \quad k = 2, \ldots, i-2, \\ d_{i+1,i-1} &= d_{i,i-2} = 0, \\ d_{i+1,i} &= d_{i,0} + d_{i,i-1} = 1 + d_{i,i-1}, \end{aligned} \tag{97}$$

for $i \geq 4$. Note that the elements of the third $(i = 2)$ and fourth row $(i = 3)$ are obtained by the same idea as

$$\begin{aligned} &d_{2,0} = 0, \quad d_{2,1} = 2, \\ &d_{3,0} = 2\tilde{h}_1 - \tilde{h}_2, \quad d_{3,1} = 0, \quad d_{3,2} = 3. \end{aligned} \tag{98}$$

References

[1] M. Abramowitz and I. A. Stegun. *Handbook of mathematical functions: with formulas, graphs, and mathematical tables*, volume 55. Courier Corporation, 1964.

[2] B. Cockburn, G. E. Karniadakis, and C.-W. Shu. The development of discontinuous galerkin methods. In *Discontinuous Galerkin Methods*, pages 3–50. Springer, 2000.

[3] G. Gassner and D. A. Kopriva. A comparison of the dispersion and dissipation errors of gauss and gauss–lobatto discontinuous galerkin spectral element methods. *SIAM Journal on Scientific Computing*, 33(5):2560–2579, 2011.

[4] G. J. Gassner. A kinetic energy preserving nodal discontinuous galerkin spectral element method. *International Journal for Numerical Methods in Fluids*, 76(1):28–50, 2014.

[5] G. J. Gassner, A. R. Winters, and D. A. Kopriva. A well balanced and entropy conservative discontinuous galerkin spectral element method for the shallow water equations. *Applied Mathematics and Computation*, 272:291–308, 2016.

[6] C. F. Gauss and C. H. Davis. *Theory of the motion of the heavenly bodies moving about the sun in conic sections*. Courier Corporation, 2004.

[7] W. Gautschi. *Orthogonal polynomials: computation and approximation*. Oxford University Press on Demand, 2004.

[8] A. Gelb, R. B. Platte, and W. S. Rosenthal. The discrete orthogonal polynomial least squares method for approximation and solving partial differential equations. *Commun. Comput. Phys.*, 3(3):734–758, 2008.

[9] H. H. Goldstine. *A History of Numerical Analysis from the 16th through the 19th Century*, volume 2. Springer Science & Business Media, 2012.

[10] S. Gottlieb, D. I. Ketcheson, and C.-W. Shu. *Strong stability preserving Runge-Kutta and multistep time discretizations*. World Scientific, 2011.

[11] S. Gottlieb and C.-W. Shu. Total variation diminishing runge-kutta schemes. *Mathematics of computation of the American Mathematical Society*, 67(221):73–85, 1998.

[12] S. Gottlieb, C.-W. Shu, and E. Tadmor. Strong stability-preserving high-order time discretization methods. *SIAM review*, 43(1):89–112, 2001.

[13] D. Huybrechs. Stable high-order quadrature rules with equidistant points. *Journal of computational and applied mathematics*, 231(2):933–947, 2009.

[14] H. T. Huynh. A flux reconstruction approach to high-order schemes including discontinuous galerkin methods. *AIAA paper*, 4079:2007, 2007.

[15] D. I. Ketcheson. Highly efficient strong stability-preserving runge–kutta methods with low-storage implementations. *SIAM Journal on Scientific Computing*, 30(4):2113–2136, 2008.

[16] D. A. Kopriva and G. Gassner. On the quadrature and weak form choices in collocation type discontinuous galerkin spectral element methods. *Journal of Scientific Computing*, 44(2):136–155, 2010.

[17] D. A. Kopriva and G. J. Gassner. An energy stable discontinuous galerkin spectral element discretization for variable coefficient advection problems. *SIAM Journal on Scientific Computing*, 36(4):A2076–A2099, 2014.

[18] D. Kosloff and H. Tal-Ezer. A modified chebyshev pseudospectral method with an o (n-1) time step restriction. *Journal of Computational Physics*, 104(2):457–469, 1993.

[19] R. J. LeVeque. *Finite volume methods for hyperbolic problems*, volume 31. Cambridge university press, 2002.

[20] D. Levy and E. Tadmor. From semidiscrete to fully discrete: Stability of runge–kutta schemes by the energy method. *SIAM review*, 40(1):40–73, 1998.

[21] J. Nordström. A roadmap to well posed and stable problems in computational physics. *Journal of Scientific Computing*, 71(1):365–385, 2017.

[22] H. Ranocha, P. Öffner, and T. Sonar. Summation-by-parts operators for correction procedure via reconstruction. *Journal of Computational Physics*, 311:299–328, 2016.

[23] W. H. Reed and T. Hill. Triangular mesh methods for the neutron transport equation. Technical report, Los Alamos Scientific Lab., N. Mex.(USA), 1973.

[24] T. Strutz. *Data fitting and uncertainty: A practical introduction to weighted least squares and beyond*. Vieweg and Teubner, 2010.